Available online at www.sciencedirect.com
ScienceDirect
Continental Shelf Research 28 (2008) 1935–1946
CONTINENTAL SHELF RESEARCH
www.elsevier.com/locate/csr

# Size sorting of fine-grained sediments during erosion: Results from the western Gulf of Lions

B.A. Law[a,b,*], P.S. Hill[b], T.G. Milligan[a], K.J. Curran[b], P.L. Wiberg[c], R.A. Wheatcroft[d]

[a]*Fisheries and Oceans Canada, Bedford Institute of Oceanography, Dartmouth, Nova Scotia, Canada B2Y 4A2*
[b]*Department of Oceanography, Dalhousie University, Halifax, Nova Scotia, Canada B3H 4J1*
[c]*Department of Environmental Sciences, University of Virginia, Charlottesville, VA 22903, USA*
[d]*College of Oceanic and Atmospheric Sciences, Oregon State University, Corvallis, OR 97331, USA*

Received 4 June 2007; received in revised form 25 October 2007; accepted 26 November 2007
Available online 3 December 2007

**Abstract**

Sediment cores from the western Gulf of Lions France were subject to known bottom shear stresses with the goal of understanding size-specific sediment erodibility. On cruises in October 2004, February and April 2005, cores with an undisturbed sediment–water interface were collected along a transect extending seaward from the Tet river mouth. The cores were exposed to increasing shear stresses (0.01–0.4 Pa) onboard the vessel shortly after collection by using a Gust erosion chamber. Samples of the suspensate were collected during the erosion experiments and analyzed for disaggregated inorganic grain size (DIGS) using a Coulter Multisizer IIe. Size-specific mobility plots were generated by dividing the proportion of each grain size in suspension at each shear stress by its proportion in the sediment before erosion. If all grain sizes that make up the bottom sediment are eroded equally from the bed, then mobility equals one for all grain sizes. Values $>1$ indicate that the suspended sediment is enriched in the size class and values $<1$ indicate that the size class is enriched in the bed. Results show that in non-cohesive, sandy silts, fine grains (clays and fine silts) are eroded preferentially from the bed at low shear stresses. With increasing bottom stress progressively larger grains are eroded from the bed. In cohesive silts, preferential erosion of the finer sizes no longer occurs, with all sizes up to medium silts eroding at approximately the same rate. Effectively, a sandy silt can be winnowed of its fine grain fraction during erosion while cohesive silts cannot. This difference in the sortability of cohesive and non-cohesive sediment during erosion may control the position and maintenance of the sand–mud transition and the sequestration of surface-adsorbed contaminants.


*Keywords:* Size-specific mobility; Erodibility; Resuspension; Gust erosion chamber; DIGS; Sortability; Sortable silt; Sand mud transition; Cohesive sediment

## 1. Introduction

Erosion and transport dynamics of cohesive sediments are important to many disciplines, yet understanding of these processes is incomplete (Black et al., 2002). Data on cohesive sediment resuspension and transport are needed by engineers to solve problems associated with water quality, navigation, and shoreline stability. Modellers also need data to calibrate key model parameters and to validate predictions (Black et al., 2002; Stevens et al., 2007). Most of the research on the resuspension of cohesive sediments has focused on bulk erosion rates and cumulative mass eroded under different stresses (e.g. Sanford and Maa, 2001; Stevens et al., 2007). Little effort has focused on measuring size-specific erosion rates. This observation gap is important to fill for several reasons. Small particles (i.e. clays and fine silts) eroded from the seabed attenuate more light per unit of mass than larger particles (i.e. coarse silts and sands) (Sheldon et al., 1972; Boss et al., 2001). They also have more surface area per unit of mass, so contaminants adsorb preferentially to them (Zwolsman et al., 1996; Milligan and Loring, 1997). Size distributions in fine sediments are an increasingly useful proxy for

*Corresponding author. Tel.: +1 902 426 8548; fax: +1 902 426 6695.
*E-mail address:* lawb@mar.dfo-mpo.gc.ca (B.A. Law).

0278-4343/$ - see front matter © 2007 Elsevier Ltd. All rights reserved.
doi:10.1016/j.csr.2007.11.006

paleocurrent intensity, as well (McCave and Hall, 2006). For these reasons, understanding of the size sorting of fine sediments during erosion is vital.

Deposition, transport, and erosion of fine sediments are fundamentally affected by aggregation (McCave, 1984; Kranck and Milligan, 1991). Aggregation is the process whereby particles adhere either by electrochemical attraction or organic bonding, thus forming large porous agglomerations called "aggregates" or "flocs". Aggregates sink much faster than the component particles within them (Sternberg et al., 1999). Therefore, settling within aggregates is responsible for the majority of deposition of fine cohesive sediments (Kranck, 1980; McCave et al., 1995; Curran et al., 2002).

Until recently the affect of aggregation on the erosion of bottom sediments has been poorly known. Thomsen and Gust (2000) used a video camera to record eroding in situ cores and showed that the resuspension of bottom sediments occurs first as aggregates. This result was later confirmed by Roberts et al. (2003) using a flume capable of eroding sediment cores in situ. The applied bottom shear stress and the sediment texture (i.e. muddy, presumably cohesive, versus sandy, presumably non-cohesive) determined if eroded aggregates persisted and if transport occurred primarily in suspension or as bedload. Roberts et al. (2003) showed that muddy, cohesive sediments were eroded and transported as suspended and bedload aggregates, whereas, sandier, non-cohesive sediments were eroded as aggregates and then broke up to be transported as single grains, predominantly as bedload. While these studies defined broadly the mode of erosion and transport, they did not elucidate the degree of size sorting that occurred.

This study examines the disaggregated inorganic grain size (DIGS) distributions of surficial sediments from high-quality cores and DIGS distributions from suspended sediments artificially eroded from those cores. These data are used to explore linkages between applied shear stress, bed texture, and size-sorting during erosion. The data are then compared to predictions of suspended size distributions based on various sediment transport models (e.g. Wiberg et al., 1994; McCave et al., 1995). The overall goal of this research is to improve predictions of size-specific sediment erosion rates.

## 2. Methods

### 2.1. Overview

As part of the US Office of Naval Research EuroStrataform program to study processes affecting the transport and accumulation of sediment on continental margins, three sampling cruises took place on the Tet margin, Gulf of Lions, France. The cruises were during October 2004 and February and May 2005. The Gulf of Lions, located in the north-west Mediterranean Sea, is a continental margin with a narrow crescent-shaped continental shelf (70 km wide) (Fig. 1). The Rhone River accounts for up to 80% of the suspended sediment ($6–10 \times 10^9$ kg/yr) delivered to the Gulf of Lions. Sediment from the Rhone is transported along the margin to the southwest, with a significant portion moving offshore through a network of submarine canyons. This study was conducted offshore of the Tet River, which delivers $\sim 6 \times 10^7$ kg sediment per year with the majority of its yearly sediment load being delivered during floods.

A transect located directly off the mouth of the Tet River was sampled extensively for sediment cores and near bottom water (Fig. 1). Seabed samples were collected using a slow-corer, which is a hydraulically damped gravity corer that preserves the sediment–water interface during sampling. It uses a 350-kg lead weight and a hydraulically damped plunger to push a 10.8-cm diameter polycarbonate core barrel into the bottom sediment (Fig. 2). Up to six replicate cores were taken at each station. In October 2004, two cores from each station were used to determine erosion thresholds and the evolution of particle size in suspension. Three cores were used during the two cruises in 2005. Erosion thresholds were determined using a Gust chamber (Gust and Muller, 1997; Tolhurst et al., 2000). The evolution of grain size was determined using an electoresistance particle size analyzer (Coulter Counter). The other cores were used to measure replicate, high-resolution porosity profiles (based on microresistivity profiling, Wheatcroft, 2002) and to determine the particle size (i.e. DIGS) of an uneroded surface for reference purposes. At each station a CTD profile was taken and a rossette sampler used to collect near-bottom water for use in the erosion experiments.

### 2.2. Gust chamber

The Gust chamber is a circular erosion device that comprises a housing with a rotating shear plate, a removable lid, and water input and output connections. It fits directly onto a slow-core tube (Fig. 2). By controlling both the rotation rate of the shear plate and the rate at which water is pumped through the device a uniform shear stress can be applied across the sediment surface. In fine sediments undergoing what is known as Type I erosion a fixed amount of sediment is available for erosion from the seabed at a given shear stress. Therefore, as suspensate with eroded bed sediment is replaced with background water, turbidity of the suspensate falls and eventually returns to background values. Shear stresses applied to cores for this study were 0.01, 0.08, 0.16, 0.24, 0.32, and 0.40 Pa, with the first step of 0.01 Pa being used to flush the tubing. Shear stress at each level was maintained for 20 min, which was sufficient in most cases for measured turbidity to return to values close to background levels. The water pumped from the chamber was collected in a 2-L flask and filtered for suspended particulate matter (SPM) and particle size analysis. The SPM data were used to determine mass of sediment eroded at each shear stress and to calibrate continuous turbidity measurements made

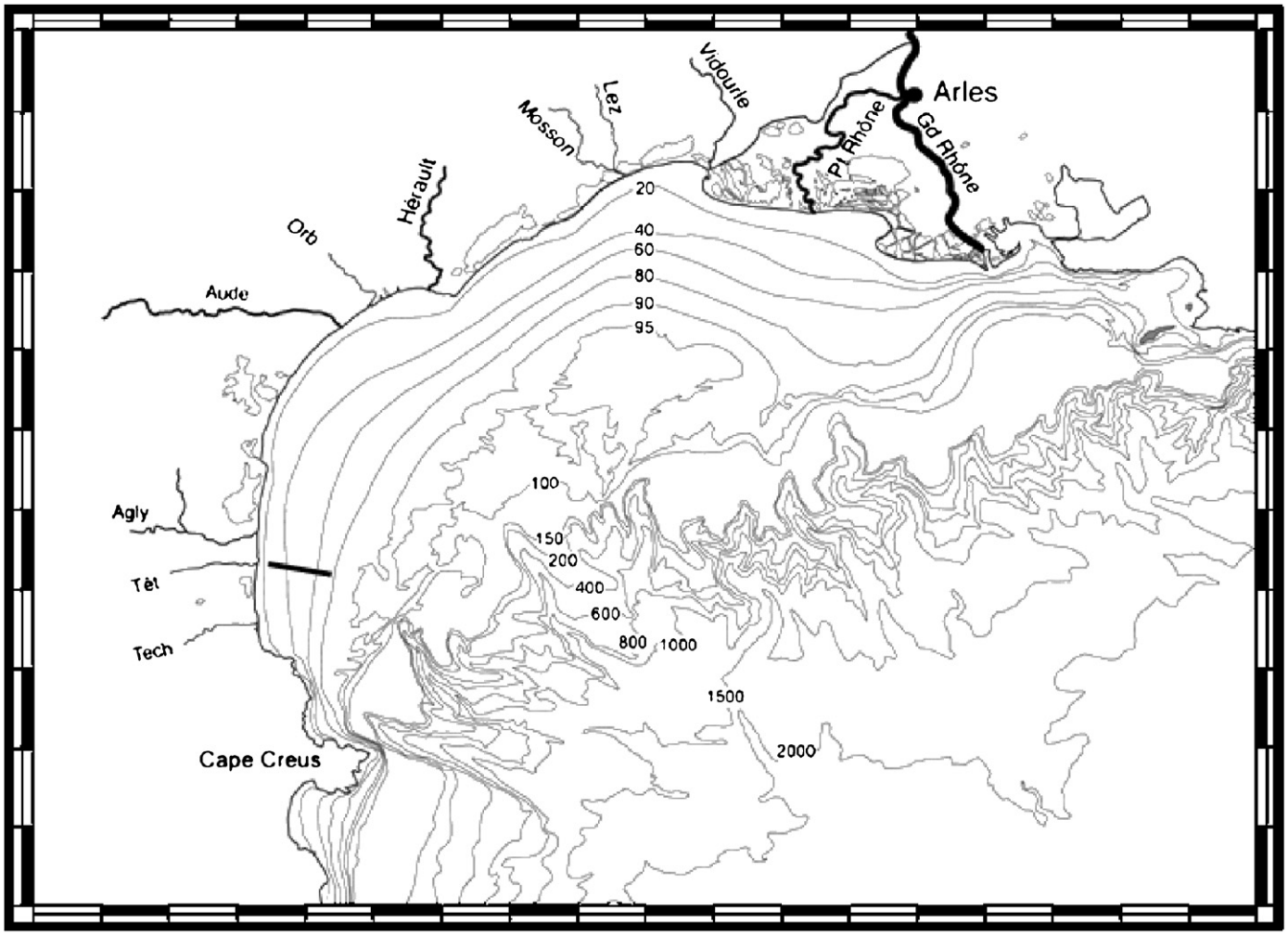


Fig. 1. A plot of the study area in the Gulf of Lions, France. The Tet River transect is marked with a black line and is labeled on the map. A transect of stations directly off the mouth at 20, 28, 35, 40, 45, 56, and 74 m water depth were extensively sampled to collect bottom cores and near bottom water samples for erosion experiments.

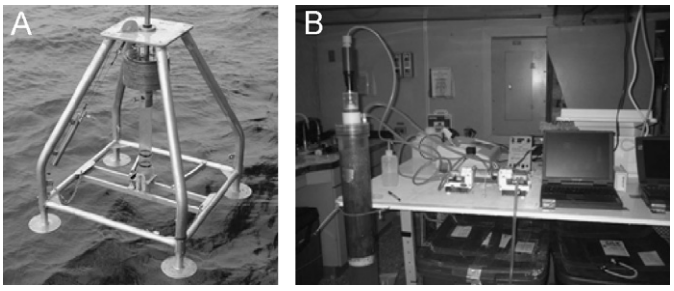


Fig. 2. (A) A photo of the hydraulically damped gravity corer (slow-corer) used to collect bottom sediment cores with an undisturbed sediment water interface. (B) A photo of the Gust microcosm erosion device used to erode the tops of collected cores under increasing shear stress steps of 0.01, 0.08, 0.16, 0.24, 0.32, and 0.40 Pa. The suspensate collected was filtered for SPM to calculate erosion rates and for grain size analysis (DIGS) on a Coulter Multisizer IIe.

with a flow-through turbidimeter. The focus of this study is size distribution of the collected suspended sediment samples as compared to the size distribution of the underlying bed sediments. For a full description of the Gust microcosm erosion device, its function, and calibration, see Gust and Muller (1997) and Tolhurst et al. (2000).

### 2.3. Particle size

The DIGS of the sediment suspended during the erosion experiments and the bottom core samples were determined using a Coulter Counter Multisizer IIe. Particle sizes are binned in a $\frac{1}{5}$ phi interval ($\phi = -\log_2 d$ ($d =$ diameter in mm) and as configured the Coulter Counter measured volume concentration in size bins covering a diameter range of 0.8–400 μm. A three tube arrangement consisting of a 30, 200 and 400 μm were used to obtain the DIGS distribution. Suspended sediment samples were analyzed for all shear stress steps at each station occupied on the Tet transect. Surficial bottom samples from the tops of cores both before and after erosion experiments were analyzed to determine the change in bed grain size after each erosion experiment. For the uneroded cores the top 0.5 cm was sampled to be consistent with the predicted depth of erosion by the Gust chamber.

*2.3.1. Suspended and bottom sediment DIGS analysis*

To determine the total SPM, known volumes of water were filtered onto millipore 8.0 μm SCWP (cellulose acetate) pre-weighed filters using standard gravimetric methods. Millipore filters were selected based on previous studies that recommend these filters because they have much lower nominal pore sizes than indicated once filtering begins, and they have excellent trapping efficiency (Sheldon, 1972). The filters were then dried at $<60\,^{\circ}C$ and weighed to obtain a sediment weight and to determine SPM concentration. For DIGS analysis samples were placed in a low temperature ($<60\,^{\circ}C$) oxygen/plasma asher to remove the filter and organic matter and to prevent the fusing together of mineral grains. Inorganic suspended sediments were resuspended in a 1% NaCl electrolytic solution before disaggregation with a sapphire-tipped ultrasonic probe prior to analysis on the Multisizer. The suspended sediment DIGS are expressed as volume/volume concentration in parts per million (ppm) and plotted as log concentration (ppm) vs. log diameter in micrometers. Organic matter was removed from bottom sediments with 35% hydrogen peroxide ($H_2O_2$). The DIGS obtained from the Multisizer are expressed as log of equivalent volume fraction (equivalent weight percent) assuming a constant particle density of $2650\,kg/m^3$ vs. log of the diameter normalized over the size range. Uncertainty in DIGS analysis is $<10\%$ which is the error in the Coulter Multisizer IIe. For a complete description of the methods of the particle size analysis used herein see Kranck and Milligan (1979) and Milligan and Kranck (1991).

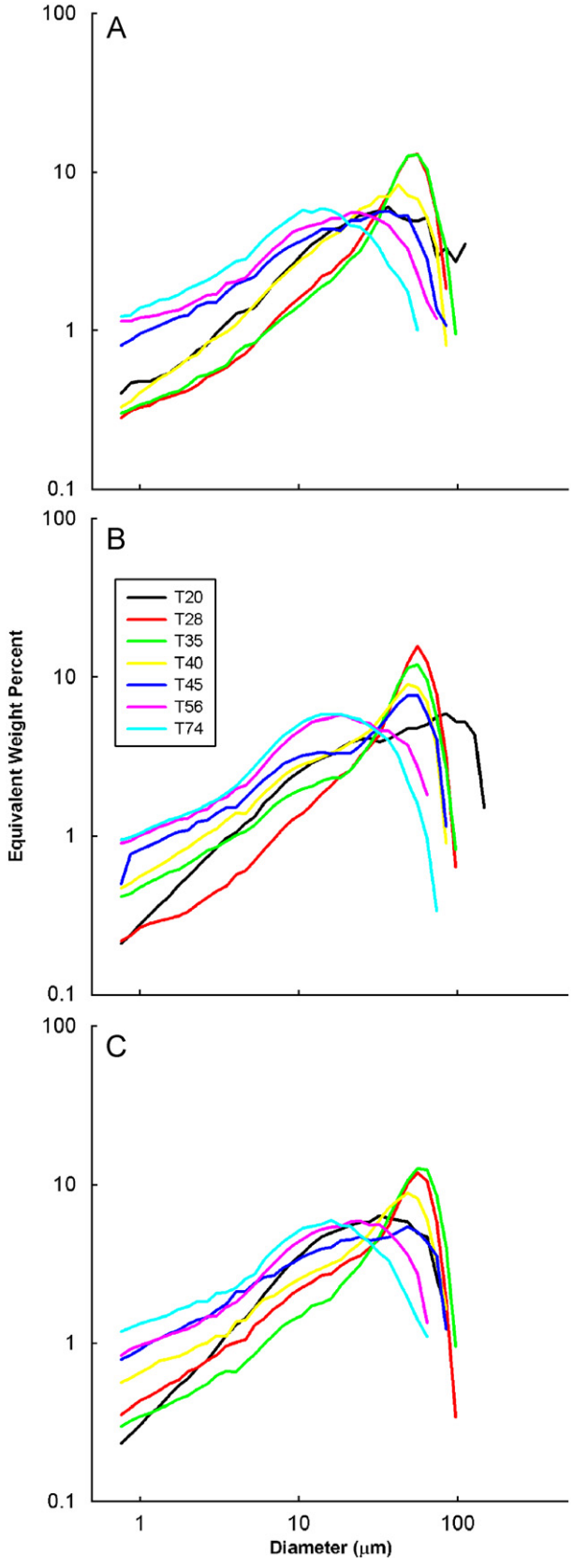


Fig. 3. A plot of the across shelf grain size collected at stations along the Tet transect during the October 2004 (A), February (B), and April (C), 2005 cruise. The DIGS distributions presented represent an average of at least two grain size curves from the analysis of uneroded core surfaces from the same station location. Expected error in DIGS spectra is assumed to be between 5% and 10% which is the error present in analyzing sediment samples with a Coulter Counter Multisizer IIe. Results show an abrupt change in DIGS spectra between station T35 and T45. Size distributions with a distinct coarse silt mode give way seaward to size distributions with mass distributed more evenly among the silts and clays.

*2.4. Determination of size specific mobility*

To quantify the size-specific sediment mobility the normalized concentration of each size class of sediment suspended by the Gust chamber for each bottom stress was divided by the corresponding normalized concentration from the top of an uneroded core at the same station. The normalized concentration from the top $<0.5\,cm$ of uneroded cores are the average DIGS spectra from at least two slo-cores from the same station location. Mobilities equal to unity indicate that the grain sizes that make up the bottom sediment are eroded equally from the bed. Values $>1$ indicate that the suspended sediment is enriched in the size class relative to the bed sediment, and values $<1$ indicate that a size class is more common in the bed than in suspension. For the purposes of this paper mobility refers to the mobility of sediments resuspended from the bed. Changes in concentration and grain size from advection and settling are removed from the mobility equation

because background concentration and grain size above the bed are subtracted for each station.

## 3. Results

The bottom sediments on the Tet transect are of mixed grain size composed primarily of muds (<63 μm diameter). Inner-shelf samples from 15 to 45 m depth had decreasing percentages of fine sand from 33% to 10%. The stations on the outer shelf beyond the 45 m isobath until the 74 m isobath (station T74), contain a small sand fraction (i.e. 2–6%) (Fig. 3; Table 1).

The across-shelf DIGS spectra (Fig. 3) show a distinct change in shape from station T35 to T45. Stations T35 shows a DIGS distribution with a coarse silt mode and a relatively minor fine silt and clay tail. The bed sediment at T45 has a larger percentage of fine sediment and lacks the distinct coarse silt mode. The greatest changes in median diameter and in the <16 μm fraction derived from DIGS spectra occur between the 35 and 45 m isobaths.

Size-specific mobilities on the Tet transect change progressively from the inner-shelf sediments, past the grain-size transition, and into the deeper water of the outer shelf. Fine silts and clays in inner-shelf sediments (e.g. stations T20, T28, T35) have high mobilities at low shear stress (Fig. 4). In other words, sediments suspended at low shear stresses are enriched in fines in comparison to the bed. As stress increases larger grains are eroded and mobilities approach values near unity at the maximum applied stress of 0.4 Pa. Near the grain-size transition at station T40 mobility values are >1 but <10, and fine sand grains are not eroded from the seabed (Fig. 4). At Station T56 and T74 mobilities are close to unity for all but the coarsest grain sizes for all increasing shear stress steps, indicating that individual grain size classes are being eroded in proportions equal to the seabed (Fig. 4).

Compared to the October 2004 and February 2005 data, mobility plots from April for the inner-shelf stations show decreases in the mobilities of finer grain sizes at lower stresses (Fig. 5). This decrease is associated with an increase in the relative proportion of fine silt and clay in the seabed. The cause of the finer texture is unknown, but could be due either to accumulation of fines during the late winter and early spring or to spatial variability in texture. Stations at or near the grain-size transition (T40) and seaward showed little or no change in mobility from October 2004 through February and April 2005, with values close to unity for all individual grain size classes eroded (Fig. 5).

Table 1
The physical characteristics of bottom sediments from the October, 2004, February, and April, 2005 sampling along the Tet transect

| | d50 (μm) | % <4 μm | % <16 μm | % <63 μm | % <63 μm | van Ledden class |
|---|---|---|---|---|---|---|
| October 2004 | | | | | | |
| T20 | 24.3 | 9.07 | 35.2 | 82.4 | 17.6 | VI |
| T28 | 38.2 | 5.57 | 20.1 | 82.9 | 17.1 | V |
| T35 | 39.9 | 5.90 | 19.3 | 79.7 | 20.3 | V |
| T40 | 25.3 | 8.36 | 33.1 | 90.7 | 9.31 | VI |
| T45 | 16.3 | 16.5 | 49.5 | 94.7 | 5.26 | VI |
| T56 | 13.3 | 19.1 | 56.8 | 97.3 | 2.71 | VI |
| T74 | 9.72 | 23.6 | 70.7 | 100.0 | 0.00 | VI |
| February 2005 | | | | | | |
| T20 | 33.2 | 7.12 | 29.4 | 67.1 | 32.9 | V |
| T28 | 43.4 | 4.52 | 16.9 | 75.8 | 24.2 | V |
| T35 | 37.5 | 8.6 | 25.9 | 81.4 | 18.6 | VI |
| T40 | 26.9 | 10.8 | 35.1 | 88.5 | 11.5 | VI |
| T45 | 22.7 | 13.9 | 41.5 | 89 | 11 | VI |
| T56 | 13.5 | 17.1 | 56.7 | 98.2 | 1.8 | VI |
| T74 | 12.2 | 15.5 | 49.1 | 93.6 | 6.4 | VI |
| April 2005 | | | | | | |
| T20 | 21.1 | 7.99 | 39.2 | 91.1 | 8.9 | VI |
| T28 | 32.0 | 8.25 | 30.8 | 81.3 | 18.7 | VI |
| T35 | 42.2 | 6.04 | 19.4 | 73.9 | 26.1 | V |
| T40 | 27.8 | 11.3 | 34.5 | 89.1 | 10.9 | VI |
| T45 | 21.0 | 16.7 | 47.9 | 90.9 | 9.1 | VI |
| T56 | 14.4 | 16.1 | 54.5 | 98.7 | 1.3 | VI |
| T74 | 11.2 | 21.6 | 65.8 | 98.9 | 1.1 | VI |

Values of d50 (median diameter), % <4 μm, % <16 μm, % <63 μm, and, % >63 μm are average values from the top of all non-eroded cores. The last column represents the classification of sediment based on van Ledden et al. (2004).

## 4. Discussion

### 4.1. Calculation of theoretical mobilities

A simplified model is used to calculate theoretical mobilities. The model assumes that for a given excess shear stress, there is a defined reference concentration at a specified reference height above bottom (cf. Smith and McLean, 1977). This approach ignores many potentially important time dependent effects in setting nearbed concentrations within the Gust chamber. It is successful, however, in reproducing the observed mobilities, and therefore is used as a tool for interpreting the observations. A comparison of various model predictions to results yields an understanding of the processes responsible for the different observed responses of mobility to increasing shear stress.

Size specific mobility is equal to the suspended sediment concentration just above the seabed divided by the concentration in the seabed. In the simplified model, the concentration in suspension immediately above the seabed is assumed to equal the reference concentration, $Ca_i$, which is proportional to the excess boundary shear stress (Smith and McLean, 1977). This concentration is calculated as (Wiberg et al., 1994)

$$Ca_i = i_b \times Cb\left(\frac{\gamma S}{1+\gamma S}\right), \quad (1)$$

where $Ca_i$ is the concentration of size class $i$ in suspension, $i_b$ is the volume fraction of $i$ in the bed sediment (normalized volume) and comes from the normalized seabed DIGS for each station, $Cb$ equals the total volume concentration of bed sediment or (2400 × (1−porosity), $S$ is

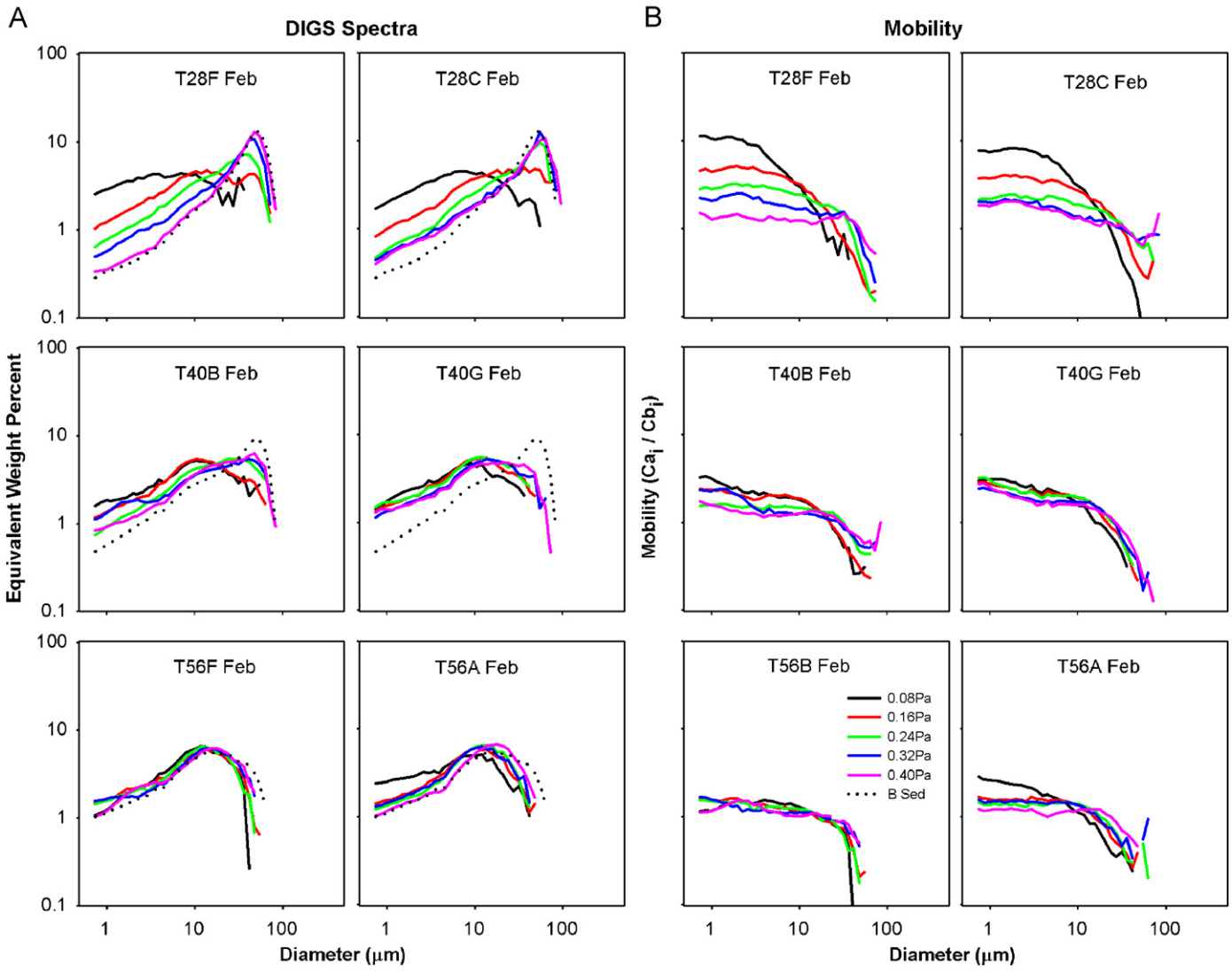


Fig. 4. (A) A plot of replicate DIGS spectra for stations T28, T40, and T56 during the February 2005 study. The black dotted line represents the average DIGS of the bottom sediment from the top <0.5 cm of cores, and the other five colored lines represent the suspended DIGS from increasing bottom shear stress generated from the Gust chamber. (B) Mobility plots of $Ca_i/Cb_i$ for increasing shear stress steps. Results show that at Station T28 fine sediment is enriched in suspension relative to the seabed when applied stresses are low. As stress increases, progressively larger grain sizes are eroded, so mobilities fall for the finer sizes and increase for the larger sizes. As the mud fraction increases moving from station T40 to T56, the marked preferential erosion of fine sediments at low shear stresses no longer occurs. Instead mobilities are similar for all but the largest grain sizes for all shear stress increments.

excess shear stress $(\tau_b-\tau_c)/(\tau_c)$, and $\gamma$ is a coefficient of resuspension. A value of 0.001 is used here (Wiberg et al., 1994). Eq. (1) can then be used to determine size specific mobility for bottom sediment:

$$Ca_{norm} = \frac{i_b \times Cb\left(\frac{\gamma S}{1+\gamma S}\right)}{\sum i_b \times Cb\left(\frac{\gamma S}{1+\gamma S}\right)}, \quad (2)$$

$$Cb_{norm} = i_b, \quad (3)$$

$$\frac{Ca_{norm}}{Cb_{norm}} = \frac{\frac{(\gamma S)}{(1+\gamma S)}}{\sum i_b \frac{(\gamma S)}{(1+\gamma S)}} = \text{size specific mobility}. \quad (4)$$

To explore possible controls on observed mobilities various models that calculate suspended sediment concentration above the seabed are used to predict size-specific mobility. Two non-cohesive sediment resuspension models and two cohesive sediment models are implemented. A third cohesive resuspension model is considered based on recent observations of the erodibility of flocs.

The first non-cohesive sediment resuspension model explored is that of Wiberg and Smith (1987). This model can be used to calculate the mobility of bottom sediments during resuspension without the effects of bed limitation. This model works with the same principal as Shields (1936) model for eroding individual grains but has better constraints on $(\tau_c)$ for small grain diameters. Essentially, the model calculates $(\tau_c)$ for the erosion of fine grain sizes from both homogeneous (well-sorted) and heterogeneous (mixed) seabeds.

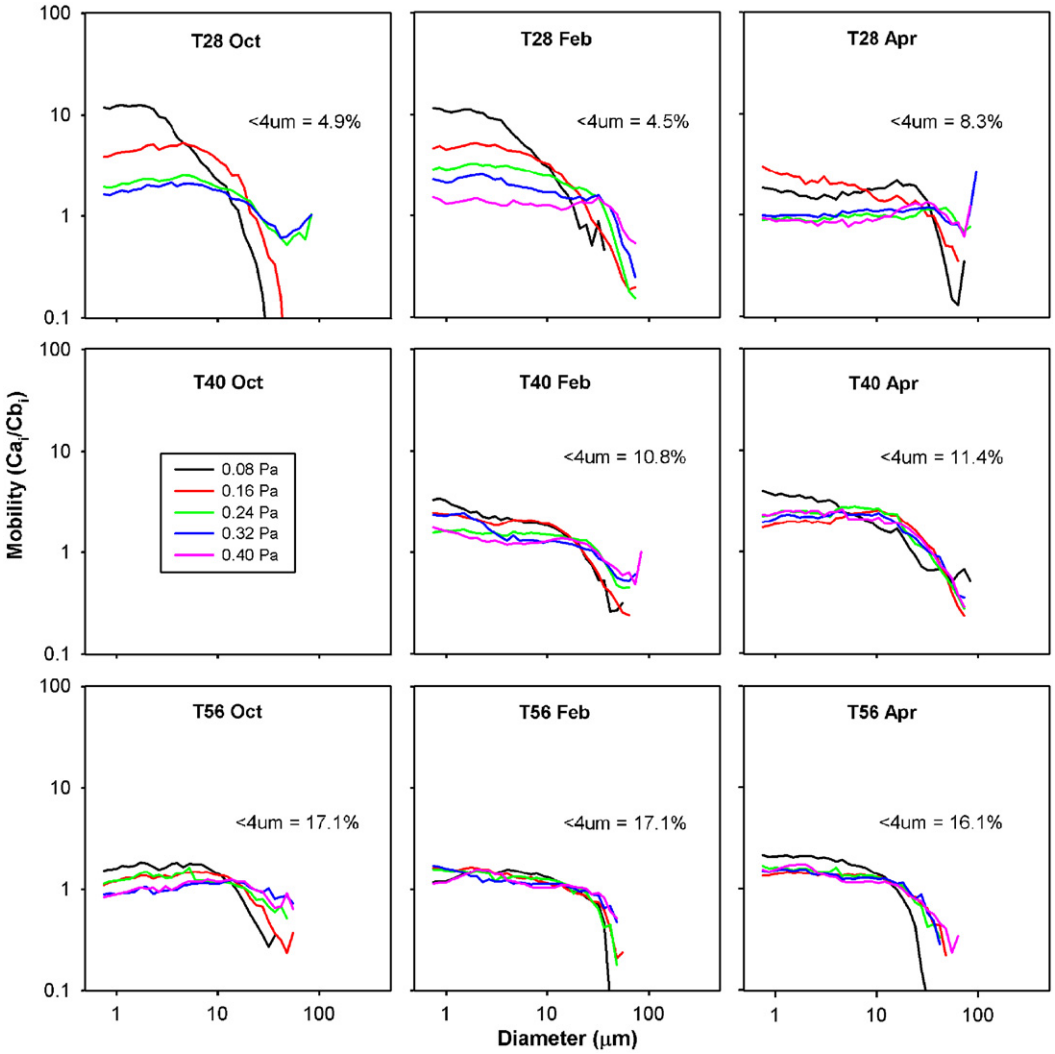


Fig. 5. A plot of the temporal evolution of mobility over the three study periods. In April at T28, preferential erosion of fine sediment at low shear stress is reduced relative to October and February. An increase in the $<4\,\mu m$ fraction at station T28 in April accompanies this change, indicating that the fines perhaps act to increase the cohesive nature of the bottom sediment. Sediments from Station T40 have similar mobilities in February and April. No cores were collected there in October. Station T56 has similar mobility over all three study periods.

The second non-cohesive resuspension model examined is the model of Wiberg et al. (1994) which introduces an "active layer depth" for erosion. This model was proposed by Wiberg et al. (1994) to reconcile time series of modeled suspended sediment concentration with observed time series of seabed stress and nearbed optical attenuation. The active layer is the layer of bed sediment that is available for resuspension. In non-cohesive sediment, as fine sediment is eroded from the seabed larger grains now in higher proportion in the seabed armor the bed and protect the remaining finer grain sizes, thereby limiting their availability for resuspension. Similarly, in undisturbed cohesive beds, consolidation of bed sediments increases over time with increasing depth below the sediment–water interface, which limits the supply of sediment available for resuspension at a given shear stress. The active layer depth for our calculations of mobility is set at 1 mm which is an approximation based on the previous erosion studies (Lynn et al., 1990; Wiberg et al., 1994).

Several authors have proposed that in cohesive sediments erodibility is equal for grains smaller than a specified size (Wiberg et al., 1994; McCave et al., 1995). As a corollary, all grains smaller than a specified size share the same critical erosion shear stress. The first cohesive model examined is that of Wiberg et al. (1994). The model uses a critical erosion shear stress of 0.1 Pa to erode all grain sizes $<40\,\mu m$ and suggests that the erosion of the seabed does not occur at lower shear stress due to the cohesive nature of fine particles. The second cohesive resuspension model discussed is that of McCave et al. (1995) which uses 10 μm as a discriminator between cohesive and non-cohesive sediments. According to the model of Wiberg and Smith (1987), $\tau_c$ for a 10 μm silt grain is 0.025 Pa, and this value is used to erode all grain sizes $<10\,\mu m$ when calculating size specific mobility with this model.

### 4.2. Model data comparison, inner (T28) vs. outer (T56) shelf sediments

#### 4.2.1. T28

The non-cohesive critical shear stresses of Wiberg and Smith (1987) coupled with Eq. (1) do not explain the mobilities found at station T28 on the Tet transect (Fig. 6). The model over-predicts the mobility of fine sediment sizes. It produces high mobilities ($\gg 1$) for fine grains and low mobilities ($\ll 1$) for larger grain sizes found in the bed sediment (Fig. 6A and B) at all shear stresses, which does not match the observed results (Fig. 6A and B).

The non-cohesive bed limitation model of Wiberg et al. (1994) predicts mobilities similar to those observed at station T28 and for the stations inshore of the grain-size transition (Fig. 6A and C). The mobilities predicted by the model show equal and high mobilities for the finest sizes at low shear stresses. As stress increases, the plateau of equal mobilities for finer sizes decreases and covers a greater range of size classes, and increasingly larger grains are resuspended. The equal mobility plateau for the fine diameters occurs for the size classes of sediment that have been completely winnowed from the active layer. At this point the total mass of small particles in suspension is equal to mass originally available in the active layer.

Mobilities predicted by the cohesive resuspension models of Wiberg et al. (1994) and McCave et al. (1995) do not resemble the observed mobilities at station T28 (Fig. 6A, D, and E). Both models predict equal mobilities for the finest size classes, but they are not high enough at low shear stresses. The plateau over which the mobilities are equal extends over too many size classes, and the plateau of equal mobilities for fine sizes does not decrease with increasing shear stresses.

In summary, at station T28 on the Tet transect the non-cohesive model of Wiberg et al. (1994) produces mobilities similar to those observed. Supply limitation from the bed is needed to limit the amount of erodible fine grain sizes. Cohesion is not needed to reproduce the observed mobilities.

#### 4.2.2. T56

The no-sediment-limitation model (Eq. (1)) with critical shear stresses from Wiberg and Smith (1987) does not do well at predicting the mobility of eroded bottom sediments at station T56, which are composed entirely of mud (Fig. 7A and B). This model over-predicts the mobility of the small grain sizes. As is the case with the T28 model prediction, this model predicts similar mobilities with increasing shear stress that do not match the observed results.

The Wiberg et al. (1994) non-cohesive supply limitation model does not predict the mobilities seen at station T56 (Fig. 7A and C). This model over-predicts the mobility of the smallest grain sizes at low shear stress. It also predicts that the diameter range of equal mobilities for fine size classes grows more with increasing shear stress than is observed.

The cohesive resuspension models of Wiberg et al. (1994) and McCave et al. (1995) both predict trends in mobility for station T56 that resemble observations. Both models predict mobilities that are near unity and equal for a large range of diameters at all shear stresses. Essentially, when muds are eroded, many grain sizes are removed from the bed simultaneously and in proportions equal to their proportions in the seabed. The model of McCave et al. (1995) is better than that of Wiberg et al. (1994) because it predicts decreasing mobilities for particles greater than 10 μm. Because Wiberg et al. (1994) use 40 μm to discriminate cohesive versus non-cohesive behavior, mobilities decrease only for particles greater than 40 μm, which does not agree with observations (Fig. 7A, D, and E). As well, the Wiberg et al. (1994) model predicts that there is no resuspension during the 0.08 Pa shear stress step, while the McCave et al. (1995) model does.

In summary, at station T56, the cohesive behavior of sediments has to be accounted for in resuspension models to reproduce observed mobilities, which is also the case for stations seaward of the grain-size transition. The model of McCave et al. (1995) works better than the Wiberg et al. (1994) model because it predicts decreasing mobilities for particles greater than 10 μm.

The erosion of consolidated sediments, as opposed to flocculated "fluff" layers (Thomsen and Gust, 2000), recently has been shown to occur at shear stress values as low as 0.04 Pa (Schaaff et al., 2006). This value of $\tau_c$ corresponds to a grain diameter of 16 μm based on the model of Wiberg and Smith (1987). A value of 0.04 Pa is also consistent with some measurements of $\tau_c$ for 10 μm grains (White, 1970). Using 0.04 Pa as the value of $\tau_c$ for all grain sizes smaller than 16 μm (or 10 μm according to White, 1970) yields predicted mobilities similar to those determined using 0.025 Pa as the value of $\tau_c$ for all grain sizes smaller than 10 μm. Mobilities using the value of $\tau_c$ yield slightly better predictions for mobility for the outer shelf stations, which are composed of predominantly mud.

This modeling exercise suggests that limits to sediment availability must be imposed in order to explain observed mobilities. Furthermore, it suggests that cohesion is responsible for the differences in observed mobilities on the Tet Transect. It is important to recognize, however, that the model is highly simplified. Future work in modeling mobility should incorporate other effects such as a stress dependent active layer thickness and the time-dependent consolidation of the bed (e.g. Wiberg et al., 1994; Sanford and Maa, 2001). For a complete list of DIGS data and mobilities collected along the Tet transect see (Law, 2007) unpublished M.Sc. thesis.

### 4.3. Cohesive sediments

Eroded cores from stations on the Tet transect show different behaviors with respect to size dependent erosion.

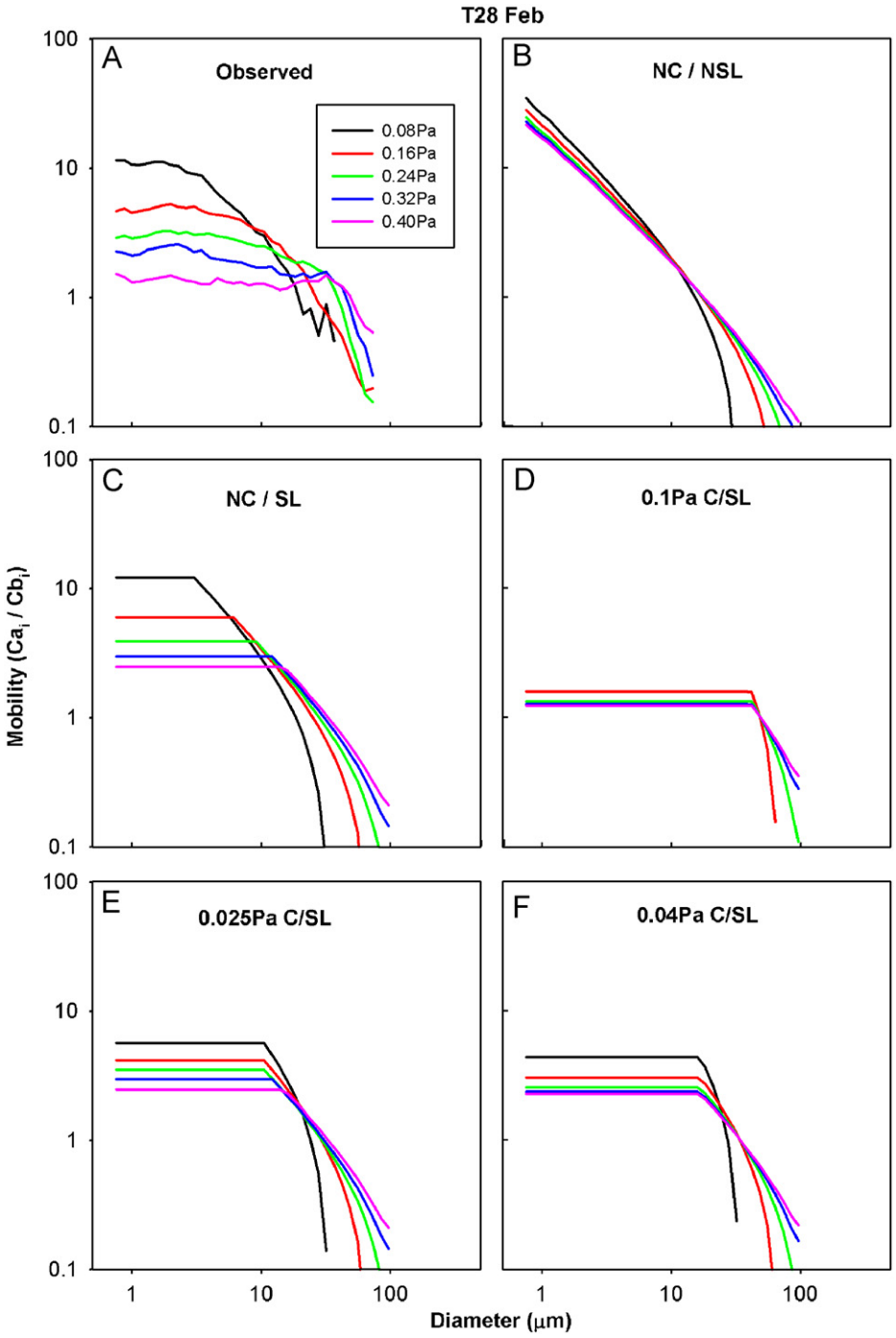


Fig. 6. Observed and theoretical sediment mobilities for Station T28 in February. Panel (A) shows mobilities generated from the observations. The remaining mobility plots were generated with simple models for the erosion of cohesive and non-cohesive sediments. Panel (B) shows mobilities for the model that is non-cohesive (NC) and imposes no supply limitation in the seabed (Eq. (1)). Panel (C) shows mobilities for the model that is non-cohesive but does impose supply limitation in the bed (also known as bed armoring; Wiberg et al., 1994). Panels (D), (E), and (F) show mobilities for the model that imposes cohesive behavior by assigning a common critical erosion shear stress to all sizes smaller than a specified value. In Panel (D) the limit is 40 μm, corresponding to a critical erosion shear stress of 0.1 Pa (Wiberg et al., 1994) for sediment erosion. For Panel (E) the limit is 10 μm, corresponding to a critical erosion shear stress of 0.025 Pa (McCave et al., 1995). In Panel (F) the limit is 16 μm, corresponding to a critical erosion shear stress of 0.04 Pa. All cohesive models also impose supply limitation in the seabed.

One set behave as non-cohesive sediments and another follow a model for cohesive sediment resuspension. Several definitions exist for distinguishing cohesive from non-cohesive sediments. The simplest is that all sediments that have mean grain sizes less than 63 μm are considered cohesive (Mignoit, 1981). Such a definition clearly does not discriminate cohesive versus non-cohesive behavior on the Tet shelf, where all of the sediments had median sizes well

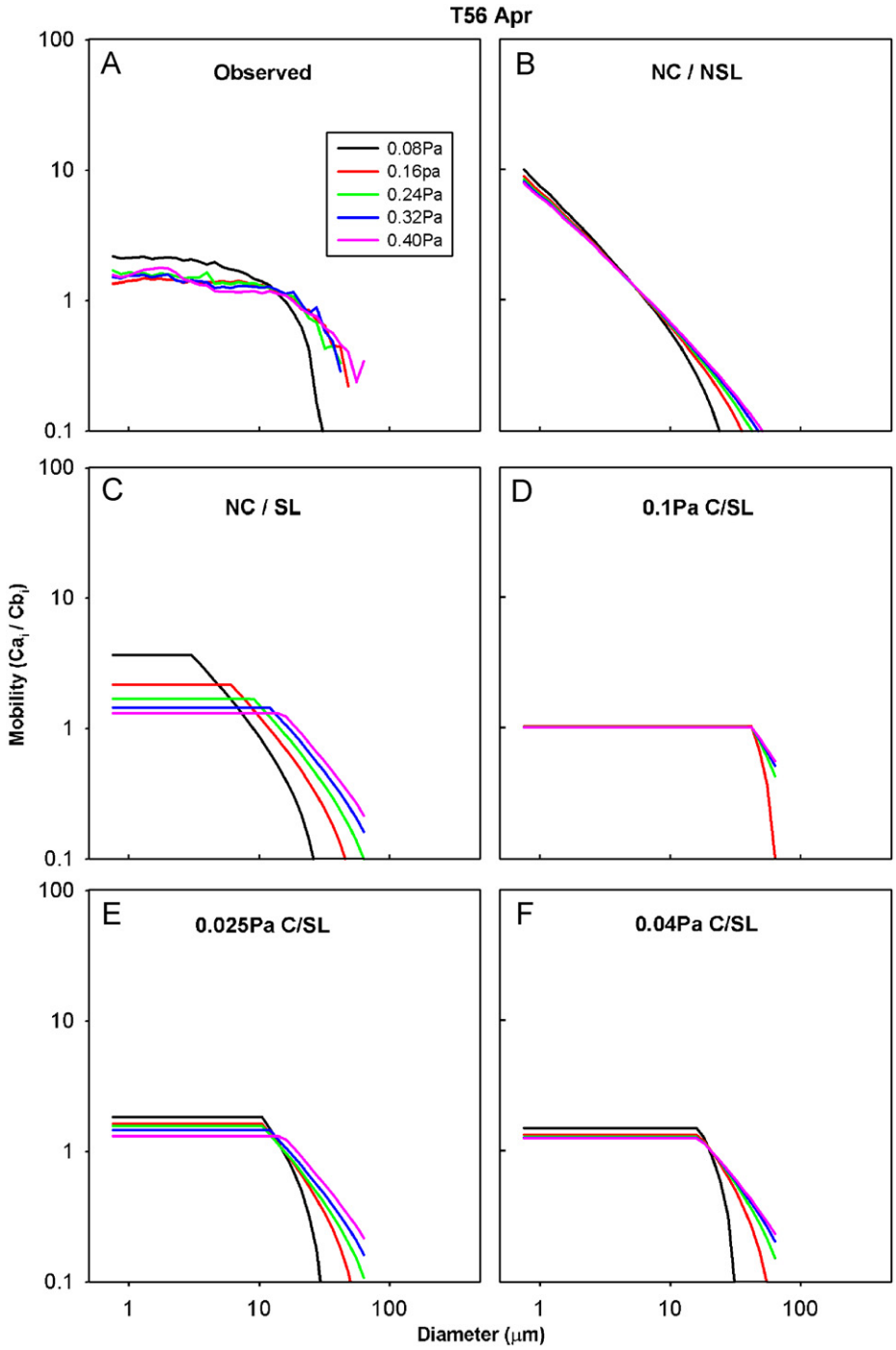


Fig. 7. Observed and theoretical sediment mobilites for Station T56 in February. Refer to the caption of Fig. 6 for details.

below 63 μm. Other definitions focus on the clay content. Mitchell (1976), Dyer (1986) and Raudkivi (1990) suggest that sediments behave cohesively when the % clay found in the sediment rises above 5–10%. More recently, Van Ledden et al. (2004) used a threshold of 7.5% clay (i.e. $<4$ μm) to distinguish cohesive and non-cohesive mixtures. They also used a sand-silt-clay ternary diagram to identify six categories of sediment based on whether the sediment matrix was supported by sand, silt, or clay and whether the sediment was cohesive or non-cohesive. Using this classification system all sediments eroded from the Tet transect fall into category V (i.e. non-cohesive, silt-dominated matrix) or VI (i.e. cohesive, silt-dominated matrix), which were divided by the 7.5% clay (i.e. $<4$ μm) boundary. The sediments eroded from the Tet transect fit the van Ledden classification scheme well. Category V non-cohesive silt mobilities followed the non-cohesive model, and category VI cohesive silt mobilities matched the cohesive model (Table 1, Figs. 5 and 6).

### 4.4. The sand–mud transition

In McCave (1972) proposed that the sand–mud transition (SMT) would form at the boundary where deposition rate of mud exceeds erosion rate by waves and currents. Recently, George et al. (2007) expanded on McCave's arguments by suggesting that at the SMT, deposition rate of mud increases because fragile flocs are no longer destroyed in the highly sheared nearbed flow. This depositional control of the SMT, however, fails to address how the mud and sand remain separated during repeated reworking by waves and currents. Results from this study show that sediment with a small percentage of clay can sort under increasing bottom shear stress, with increasingly coarser grains being suspended at increasing stresses. In sediments that contain $>7.5\%$ clay, a wide range of sizes are eroded at equal rates. Sediments with a small clay fraction can be winnowed during erosion, but sediments with a larger clay fraction cannot. With this mechanism an integrated conceptual model of the formation and maintenance of the SMT emerges.

To produce a deposit with high clay content, a suspension must be flocculated during deposition. Otherwise, the small settling velocities of clay-sized grains makes their settling flux vanishingly small relative to larger grain sizes. As a result, deposits with a high clay content form where nearbed shear is low enough to allow flocs to survive intact as they settle to the seabed. The abruptness of the SMT arises initially because the extent of flocculation diminishes rapidly with increasing boundary shear stress (Hill et al., 2001). After a single erosion–deposition event, sediment seaward of the SMT has a high clay content because it deposited as flocs. Sediment landward of the SMT has a low clay content because it deposited as single grains. With the arrival of the next transport event, the sediment with low clay content is winnowed of its fine fraction, and the sediment with a high clay content is transported en masse. This differential sorting of the sediment landward and seaward of the SMT accentuates the abruptness of the boundary.

Future work in different locations will clarify the effect of grain size on sortability. The Tet River transect was one where the sediment delivery is low and occurs mostly during flood events. During the time of the study, however, there was never a large influx of inorganic material. Sortability studies in an area with large sediment delivery and distinct SMT will help clarify a definition for cohesive versus non-cohesive sediment behavior. As mud is deposited it may change the mobility of a bottom sediment and overwhelm the possibility of winnowing its fine grain fraction. Also, if fine grains can be winnowed from sandy environments and removed from muddy beds at low shear stress, implications for contaminant transport exist. Trace metals and other surface reactive contaminants such as PAH's and PCB's have been shown to have a high affinity for the large surface area of smaller grain sizes. If sediments are exposed to conditions favorable for resuspension and contain harmful contaminants then transport of these materials may occur even at low shear stress.

## 5. Conclusion

Non-cohesive, sandy-silts are prone to sorting because at low shear stresses the clay and fine silt can be winnowed from the sand and coarse silt. Observed mobilities are best predicted by the model of Wiberg et al. (1994) for the stations with low clay content landward of the grain size transition. In contrast, when the fraction of clay, $<4\,\mu m$, in a bottom sediment rises above approximately 7.5%, the mobility of that sediment approaches 1 across all grain size classes. When eroded, cohesive sediments transport a wide range of grain sizes in suspension in equal concentration proportion to the seabed, even at low shear stress. Effectively, as shear stress increases, so does the mass of sediment eroded, yet the size distribution of sediment in the seabed remains relatively unchanged.

Studies on cohesive sediment transport have shown evidence for the erosion of consolidated bottom sediments at 0.04 Pa, which is equal to the stress required to erode a $16\,\mu m$ sediment grain based on the work of Wiberg and Smith (1987). Modeled mobilities using $16\,\mu m$ as the minimum size for sortable silt are closest to observations. More work will indicate whether this diameter cutoff for "sortability" should be used in place of the $10\,\mu m$ cutoff proposed by McCave et al. (1995) in cohesive transport models.

The difference in the ability to sort cohesive and non-cohesive sediment during erosion may prove to be an important control on the position and maintenance of the SMT. Non-cohesive muddy sands can have their fine fraction removed at low shear stresses, whereas cohesive sandy muds undergo little sorting, thus maintaining their muddy character.

## Acknowledgments

This research was supported by the US Office of Naval Research (ONR) Contracts, N00014-04-1-0165 and N00014-04-1-0182, awarded to P.S. Hill and T.G. Milligan. Sincere thanks are given to Sarah Lawson and Adam Meurer for use and help with the Gust chamber. Thanks are given to Andrew Stevens and Tina Drexler for help in sample collection and all other scientists that participated during the three cruises and made the time at sea and on land enjoyable (Café de Rance). Special thanks are given to the captain and crew of the *RV Oceanus* and *RV Endeavor* from WHOI and URI, respectively. The authors appreciate the helpful comments from three anonymous reviewers.

## References

Black, K.S., Tolhurst, T.J., Paterson, D.M., Hagerthy, S.E., 2002. Working with natural cohesive sediments. Journal of Hydraulic Engineering 128, 2–8.

Boss, E., Twardowski, M.S., Herring, S., 2001. The shape of the particulate beam attenuation spectrum and its relation to the size distribution of oceanic particles. Applied Optics 40, 4885–4893.

Curran, K.J., Hill, P.S., Milligan, T.G., 2002. Fine-grained suspended sediment dynamics in the Eel River flood plume. Continental Shelf Research 22, 2537–2550.

Dyer, K.R., 1986. Coastal and Estuarine Sediment Dynamics. Wiley, Chichester.

George, D.A., Hill, P.S., Milligan, T.G., 2007. Flocculation, heavy metals (Cu, Pb, Zn) and the sand–mud transition on the Apennine Margin, Italy. Continental Shelf Research 27, 475–488.

Gust, G., Muller, V., 1997. Interfacial hydrodynamics and entrainment functions of currently used erosion devices. In: Burt, N., Parker, R., Watts, J. (Eds.), Cohesive Sediments. Wiley, Chichester, UK, pp. 149–174.

Hill, P.S., Voulgaris, G., Trowbridge, J.H., 2001. Controls on floc size in a continental shelf bottom boundary layer. Journal of Geophysical Research 106, 9543–9549.

Kranck, K., 1980. Experiments on the significance of flocculation in the settling of fine-grained sediment in still water. Canadian Journal of Earth Sciences 17, 1517–1526.

Kranck, K., Milligan, T.G., 1979. The use of Coulter Counters in studies of particle size distributions in aquatic environments. Report Series/BI-R-79-7/November, p. ii+48.

Kranck, K., Milligan, T.G., 1991. Grain size in oceanography. In: Syvitski, J.P.M. (Ed.), Principles, Methods, and Application of Particle Size Analysis. Cambridge University Press, New York, pp. 332–345.

Law, B.A., 2007. Size sorting of fine-grained sediments during erosion. Unpublished M.Sc. Thesis, Dalhousie University.

Lynn, V.D., Butman, B., Grant, W.D., 1990. Sediment movement along the US east coast continental shelf—II. Modeling suspended sediment concentrations and transport rates during storms. Continental Shelf Research 10, 429–460.

McCave, I.N., 1972. Transport and escape of fine-grained sediment from shelf areas. In: Swift, D.J.P., Duane, D.B., Pilkey, O.H. (Eds.), Shelf Sediment Transport: Process and Pattern. Dowden, Hutchinson and Ross, pp. 225–247.

McCave, I.N., 1984. Size spectra and aggregation of suspended particles in the deep ocean. Deep Sea Research 31, 329–352.

McCave, I.N., Hall, I.R., 2006. Size sorting in marine muds: processes, pitfalls, and prospects for paleaoflow-speed proxies. Geochemistry, Geophysics, and Geosystems 7 (Q10N05; 37pp.).

McCave, I.N., Manighetti, B., Robinson, S.G., 1995. Sortable silt and fine sediment size/composition slicing: parameters for palaeocurrent speed and palaeoceanography. Paleoceanography 10 (3), 593–610.

Mignoit, C., 1981. Estuarine sediment dynamics—cohesive and non-cohesive materials, vol. 6(4). Defence Research Information Center, Orpington, UK, pp. 359–432.

Milligan, T.G., Kranck, K., 1991. Electroresistance particle size analyzers. In: Syvitski, J.P.M. (Ed.), Principles, Methods, and Application of Particle Size Analysis. Cambridge University Press, New York, pp. 109–118.

Milligan, T.G., Loring, D.H., 1997. The effect of flocculation on the size distributions of bottom sediment in coastal inlets: implications for contaminant transport. Water, Air, and Soil Pollution 99, 33–42.

Mitchell, J.K., 1976. Fundamentals of Soil Behaviour. University of California, Wiley, Berkeley.

Raudkivi, A.J., 1990. Loose Boundary Hydraulics, third ed. Pergamon Press, Oxford.

Roberts, J.D., Richard, J.A., James, S.C., 2003. Measurements of sediment erosion and transport with the adjustable shear stress erosion and transport flume. Journal of Hydraulic Engineering 129, 862–871.

Sanford, L.P., Maa, J.P.Y., 2001. A unified formulation for fine sediments. Marine Geology 179, 9–23.

Schaaff, E., Grenz, C., Pinazo, C., Lansard, B., 2006. Field and laboratory measurements of sediment erodibility: a comparison. Journal of Sea Research 55, 30–42.

Sheldon, R.W., 1972. Size separation of marine seston by membrane and glass-fiber filters. Limnology and Oceanography 17, 494–498.

Sheldon, R.W., Prakash, A., Sutcliffe Jr., W.H., 1972. The size distribution of particles in the ocean. Limnology and Oceanography 17, 327–339.

Shields, A., 1936. Application of the theory of similarity and turbulence research to bedload movement. Mitteilungen aus dem Preussischen Versuchsanstalt fuer Wasserbau und Schiffbau 26, 5–24.

Smith, J.D., McLean, S.R., 1977. Spatially averaged flow over a wavy surface. Journal of Geophysical Research 82, 1735–1746.

Sternberg, R.W., Berhane, I., Ogston, A.S., 1999. Measurement of size and settling velocity of suspended aggregates on the Northern California continental shelf. Marine Geology 154, 43–54.

Stevens, A.W., Wheatcroft, R.A., Wiberg, P.L., 2007. Sediment erodibility along the western Adriatic Margin, Italy. Continental Shelf Research 27, 400–416.

Thomsen, L., Gust, G., 2000. Sediment erosion thresholds and characteristics of resuspended aggregates on the western European continental margin. Deep-Sea Research, Part I 47, 1881–1897.

Tolhurst, T.J., Black, K.S., Paterson, D.M., Mitchener, H.J., Termatt, G.R., Shayler, S.A., 2000. A comparison and measurement standardization of four in situ devices for measuring the erosion shear stress of intertidal sediments. Continental Shelf Research 20 (10–11), 1397–1418.

Van Ledden, M., van Kesteren, W.G.M., Winterwerp, J.C., 2004. A conceptual framework for the erosion behavior of sand–mud mixtures. Continental Shelf Research 24, 1–11.

Wheatcroft, R.A., 2002. In situ measurements of near-surface porosity in shallow-water marine sediments. IEEE Journal of Oceanic Engineering 27, 561–570.

White, S.J., 1970. Plane bed thresholds of fine grained sediments. Nature 228, 152–153.

Wiberg, P.L., Smith, D.J., 1987. Calculations of the critical shear stress for motion of uniform and heterogeneous sediments. Water Resources Research 23, 1471–1478.

Wiberg, P.L., Drake, D.E., Cacchione, D.A., 1994. Sediment resuspension and bed Armoring during high bottom stress events on the northern California inner continental shelf: measurements and predictions. Continental Shelf Research 14 (10–11), 1191–1219.

Zwolsman, J.J.G., van Eck, G.T.M., Burger, G., 1996. Spatial and temporal distribution of trace metals in sediments from the Scheldt Estuary, South-west Netherlands. Estuarine and Coastal Shelf Science 43, 55–79.